

Improved Virtual Force Algorithm based on the States of Matter for Improving Coverage of Mobile Wireless Sensor Networks

Vahid Kiani¹  and Azadeh Soltani²

Department of Computer Engineering, University of Bojnord, Bojnord¹
University of Bojnord, Bojnord²
Corresponding author's email: vkiani@ub.ac.ir

Article Info

Article type:
Research Article

Article History:
Received 2022-01-03
Received in revised form:
2022-05-02
Accepted 2022-06-23
Published online:
2022-07-13

Keywords:
Coverage improvement,
Maximal coverage,
Sensor placement,
States of matter,
Virtual force algorithm.

ABSTRACT

Sensor placement is a critical issue in wireless sensor networks that affects the quality of wireless sensor network coverage. In this paper, we propose an improved virtual force algorithm based on the states of matter (IVFASM) for relocating sensors of a mobile wireless sensor network. IVFASM simulates the behavior of molecules in different states of matter to improve the coverage of sensors. In the proposed IVASM algorithm, the strength of repulsive forces, the kinetic energy of the matter molecules, and attraction radius are dynamically adjusted over time according to different states of matter. As a result, in the gaseous state, sensors move rapidly apart; in the liquid state, sensors absorb each other to fill small holes gradually; in the solid state, sensors stabilize their final position. In the simulation, different states of matter led to improved coverage and fewer holes. Evaluation of the proposed method on 14 sample problems with the different numbers of sensors and comparison of the results with state of the art revealed that the proposed method can achieve a higher coverage rate in almost all sample problems. For a sample problem of 30 sensors, genetic algorithm (GA) and particle swarm optimization (PSO) achieved a coverage ratio of 69%, fuzzy redeployment algorithm (FRED) achieved a coverage ratio of 72%, classical virtual force algorithm (VFA) obtained a coverage ratio of 79%, improved virtual force algorithm based on area intensity (IVFAI) achieved a coverage ratio of 82%, and our proposed method IVFASM achieved a coverage ratio of 83%.

I. Introduction

Wireless sensor networks (WSNs) are constituted by several sensor nodes spatially distributed in a target geographic area [1]–[4]. A common usage of WSNs is monitoring events in the target area including the presence or movement of any objects. WSNs have a wide range of applications, including military applications [5], [6], environmental monitoring [7], [8], industrial monitoring [9]–[11], agricultural monitoring [12]–[15], remote healthcare [16], [17], and target detection and tracking [18]–[21]. The main goal of WSN is decision-making or knowledge acquisition based on information gathered from sensors. In a cluster-based WSN, each sensor sends its sensing

information to the cluster-head after local processing [22]–[24]. The cluster-head may identify events or monitor targets based on the data obtained from sensors within the cluster. For example, WSN may be used on the battlefield for enemy monitoring and surveillance. Each sensor monitors its neighborhood area within a fixed sensing radius and sends a signal to the cluster-head if it recognizes an unidentified object. By combining received information from sensors, the cluster-head can detect and track combat objectives on the battlefield.

Sensor deployment is one of the most important issues in wireless sensor networks, which affects many factors including coverage, communication costs, and energy



consumption of the sensors [25]–[27]. The performance of a wireless sensor network largely depends on the coverage provided by the sensor network [28], [29]. Coverage substantially affects how well WSN monitors all local regions in a vast target area, and how efficiently a sensor network can identify moving targets. Therefore, the sensors should be placed in such a way that they monitor all regions of the target area uniformly and maximize the sensing capability of the network.

Sensor deployment methods are classified into deterministic and random [2]. Deterministic deployment is used for sensor placement in friendly and accessible environments [30]. In this approach, sensors are deployed based on a specific geometric pattern. On the other hand, random deployment is often used for sensor placement in wildlife, hostile, unsafe, or vast target areas. In this case, sensors are randomly deployed in the environment with a device such as an airplane [2], [31]. Random deployment does not provide uniform coverage of the target area and could cause some areas to have a high density of sensors while others are not covered [3]. Moreover, battery depletion can also lead to coverage holes during network operation. Accordingly, coverage improvement algorithms are applied to the initial deployment and modify the position of sensors to provide maximum coverage, remove holes, and uniformly cover the entire target area.

This paper focuses on the coverage improvement problem that aims to enhance the deployment of sensors for a given set of sensors randomly pre-deployed in a region of interest. Unlike methods that provide full coverage while minimizing the number of sensors, in the coverage improvement problem, the number of sensors is constant, and the goal is to redeploy sensors so that the maximum extent of the target area is covered [3], [32]. Coverage improvement of mobile wireless sensor networks is an NP-hard problem and cannot be exactly solved in a limited time [33].

In addition to coverage maximization [1], [34], sensor redeployment algorithms may consider other goals such as connectivity of the sensor network [35], [36], battery power consumption during placement [26], reducing the energy consumption of the entire network while monitoring the area [27], and uniform distribution of sensors [37]. A popular algorithm for enhancing coverage of WSN is the Virtual Force Algorithm (VFA), which is based on the theory of virtual force and considers the attractive and repulsive forces between molecules [38]. Zou et al. proposed VFA to optimize the positioning of sensors and maximize the coverage in cluster-based WSNs [38]. The following assumptions are considered in a cluster-based sensor network [38]:

- Each sensor can sense the environment, perform limited calculations, communicate with the cluster head, and move to a new location.
- After the initial random placement of sensors, all sensor nodes can communicate with the cluster

head.

- The cluster head is responsible for receiving all node positions and executing the sensor placement algorithm and sending the desired position to all sensors.
- During the execution of the sensor deployment algorithm, sensors do not move. Each sensor moves to its final location in one movement after execution is complete and the final placement is determined.

In this paper, we propose an improved virtual force algorithm based on the states of matter (IVFASM), that considers sensors as molecules and adjusts the intensity of the attractive and repulsive forces between molecules, the kinetic energy of molecules, and the attraction radius of molecules in different states of matter (gas, liquid, and solid). Accordingly, IVFASM consists of three phases each of which simulates the behavior of the sensors differently. IVFASM first assumes that the matter is in the gas state and the sensors can move a large allowable distance. The algorithm then enters the liquid state, in which sensors have some kind of adhesion in their motion. In this phase, the strength of the attractive force between the sensor nodes does not change, but the strength of repulsive force will reduce, and the motion of the sensors becomes limited. Finally, the state of matter is considered solid. In the solid state, molecules strongly absorb each other and sensors vibrate locally to stabilize their final location.

The rest of this paper is organized as follows. Related work is briefly reviewed in Section II. Section III provides the problem statement. Section IV describes the virtual force algorithm. In Section V, the proposed IVFASM algorithm is introduced. Experimental results are presented in Section VI. The paper is concluded in Section VII.

II. Literature Review

The researchers introduced numerous approaches to address the coverage improvement problem for mobile wireless sensor networks that monitor a target area. Howard et al. were the first who considered virtual forces between sensors of WSN and improved network coverage by simulating repulsive forces between sensors. They proposed a potential force-based algorithm to improve coverage of WSN that is inspired by the theory of electric potential fields and repulsive forces between them [39]. Zou et al. then completed this idea and proposed the virtual force algorithm (VFA) for coverage maximization that applies attractive forces alongside repulsive forces between sensors [38]. As the most effective coverage improvement algorithm, the VFA was then improved by many scholars. A summary of these research works is given in Table I.

Wang et al. combined the VFA with the particle swarm optimization algorithm (VFPSO) and included virtual forces of sensor nodes in calculating the velocity vector in PSO [40]. Song et al. combined the VFA with the biogeography-based optimization algorithm (VFBBO) [41]. They added the

attraction, repulsion, and boundary binding techniques from VFA to the BBO algorithm.

TABLE I
SUMMARY AND COMPARISON OF RELATED WORKS

Author	Year	Method	Advantages	Disadvantages
Howard [39]	2002	artificial potential fields algorithm (PFA)	decentralized redeployment, obstacles avoidance, low communication, scalability	only considers repulsive forces, may not fill holes
Zou [38]	2004	virtual force algorithm (VFA)	decentralized redeployment, low computation time, obstacles avoidance, the combination of repulsive and attractive forces	fixed value for optimal distance, sensors collision can happen, discrete coordination system
Wang [40]	2007	virtual force particle swarm optimization (VFPSO)	improves convergence speed of PSO, avoids local optima	centralized redeployment, lower speed than VFA and PFA
Song [41]	2013	virtual force biogeography-based optimization (VFBBO)	improves convergence speed of BBO, avoids local optima	centralized redeployment, lower speed than VFA and PFA
Yang [37]	2013	hybrid local virtual force algorithm (HLVFA)	pays attention to the local density of sensors, improves the uniformity of final deployment, adds a local density force	has no global understanding of the distribution of sensors
Li [25]	2015	modified energy balanced virtual force algorithm (MVFA)	balanced energy distribution among sensor nodes, improves uniformity, less energy consumption, adds a balancing force	is not applied to heterogeneous mobile sensor networks with various sensing ranges
Umadevi [42]	2018	two-phase virtual force and particle swarm optimization algorithm	lower average moving distance by sensor matching using PSO, reduces energy consumption	centralized deployment, final matching would be done by the cluster head
Deng [43]	2019	improved virtual spring force algorithm (VFASF-OPT)	avoids holes in final deployment, adds an external central force to spring forces, lower energy consumption	sensor communication and data transmission have not been considered, computational complexity
Xie [44]	2019	improved virtual force algorithm based on area intensity (IVFAI)	improves coverage ratio, reduces computation time, adjusts optimal distance based on area intensity, adjusts coefficients of attractive and repulsive forces for each sensor	sensitive to correct adjustment of parameters, proposed parameter adjustment methods that do not always produce good results
Wang [45]	2019	virtual-force-lévy-embedded grey wolf optimization (VFLGWO)	improves coverage ratio, higher uniformity, lower average moving distance by sensor matching, combines virtual force and gray wolf optimization	centralized deployment, higher computational complexity than VFA, lower scalability
Liu [46]	2020	virtual molecular force algorithm (VMFA)	improves coverage ratio, higher uniformity, lower average moving distance by sensor matching, combines virtual force and gray wolf optimization	centralized deployment, higher computational complexity than VFA, lower scalability
Qi [47]	2021	resampling particle swarm optimization algorithm embedded with virtual force (RPSODV)	improves coverage ratio, faster convergence, considers boundary forces, combination with resampling PSO	centralized deployment, higher computational complexity than VFA, lower scalability
Yao [48]	2021	virtual force-directed ant lion optimization algorithm (VFIALO)	removes holes, improves coverage ratio, considers boundary forces, combines virtual forces with the ant-lion algorithm	centralized deployment, higher computational complexity than VFA, lower scalability
Wen [49]	2022	vampire bat algorithm combined with improved virtual force (VBIVFA)	removes holes, reduces energy consumption, lower moving distance	centralized deployment, higher computational complexity than VFA, lower scalability
Our Method	2022	improved virtual force algorithm based on states of matter (IVFASM)	improves coverage, fast computation, adjusts the optimal distance, dynamic adjustment of attractive and repulsive forces coefficients	no additional forces are considered

Yang et al. proposed a hybrid local virtual force algorithm (HLVFA) [37]. In addition to the attractive and repulsive forces in the VFA, they suggested considering a repulsive

force based on the local density of sensors to improve uniformity alongside coverage. Li et al. proposed modified energy balanced virtual force algorithm (MVFA) that uses an

energy control function to evenly distribute the remaining energy of sensor nodes during redeployment [25]. In a hybrid approach, Umadevi et al. utilized the VFA in the first phase and the PSO algorithm in the second phase to improve the placement of sensors in the wireless sensor network [42]. Deng et al. introduced the improved virtual spring force algorithm (VFASF-OPT), in which, sensor deployment begins from the center of the target area and other sensor nodes are gradually added to the outer region [43]. Xie et al. proposed the improved virtual force based on area intensity (IVFAI) and adjusted the optimal distance of each sensor based on the intensity of neighboring sensors in its local neighborhood [44]. They also determined proper values for attractive and repulsive force coefficients for every sensor independently from others. Wang et al. combined virtual force with Lévy-embedded Grey Wolf Optimizer (VFLGWO) to effectively improve the coverage of a wireless sensor network [45].

Liu et al. in [46], based on the basic idea of air molecular theory, proposed the virtual molecular force algorithm (VMFA) to improve coverage of sensor deployment. Their method tracks the trajectory of each sensor movement over time and stops moving the sensor if all forces applied to it from neighboring sensors are small enough. They assumed that there is an interaction between nodes in the mobile sensor network, and the resultant force of these forces constitutes the resultant force network of sensor nodes in the monitoring area, which drives the sensor nodes to move to their corresponding location. Qi et al. in [47] proposed the resampling particle swarm optimization algorithm embedded with virtual force (RPSODV) to maximize coverage and reduce sensor movements. They considered also repulsive forces between sensors and repulsive forces from boundaries to improve coverage. Yao et al. in [48] proposed the virtual force-directed ant lion optimization algorithm (VFIALO) to avoid the ant-lion algorithm falling into local optima, accelerate its convergence speed, and improve its global optimization ability. In the virtual force part of their proposed method three forces including neighbor node forces, grid points gravity, and boundary repulsion are mixed. A higher coverage ratio was obtained by their method compared with VFA, VF-PSO, and the classical ant-lion algorithm. Wen et al. in [49] proposed a vampire bat algorithm combined with improved virtual force (VBIVFA). In their method, a bipartite graph model is first created between sensor nodes and cellular grid points. Then vampire bat algorithm is employed for bipartite graph matching, and improved virtual force is applied after that for further improvement in coverage.

Some other researchers extended the virtual force algorithm to consider security issues, priorities, and computational geometry. Bartolini et al. in [50] studied vulnerabilities of the virtual force algorithm (VFA) against opportunistic movement attack, where an attacker tries to influence the movement of other sensors and prevent uniform coverage of the target area.

They proposed two algorithms to counterattack the opportunistic movement attack. Kalayci et al. in [51] proposed a genetic algorithm for sensor deployment to maximize coverage and have not considered an initial input deployment to be improved by the algorithm. Their algorithm is designed for non-homogeneous areas where the target monitoring area is divided into several parts and priorities are attached to these parts. They also assumed that the sensors should be 1-connected to each other and some bot spot areas in the target environment should be covered by at least k sensors (k -covered). Mahboubi and Aghdam in [52] proposed a virtual force algorithm based on the Voronoi diagram that attempts to improve coverage of WSN for a target area. They considered some additional virtual forces that are applied to the sensor from the vertices and boundaries of the target area. The new location of the sensor is computed by the vector sum of the virtual forces of vertices and boundaries. They only moved the sensor to the new location if coverage increases.

Although many research works have focused on improving the virtual force algorithm, none of these studies has paid attention to modeling the states of matter. This paper proposes an improved virtual force algorithm based on the nature of molecules in various states of matter to improve the coverage of wireless sensor networks.

III. Problem Statement

The problem of coverage improvement for mobile wireless sensor networks is defined in this section. In this study, as shown in Fig. 1, the coverage range of each sensor is assumed to be a circle with a fixed radius r based on the binary sensor model. Every target in the sensing radius of the sensor will be detected by the sensor with complete certainty. To evaluate the coverage rate of WSN in a two-dimensional area, the target area is often divided into n_{total} points in a regular grid. If the WSN can cover $n_{covered}$ points, the coverage rate is estimated as follows [44]:

$$R_c = n_{covered}/n_{total} \quad (1)$$

Consider N sensors ($S = \{s_1, s_2, s_3, \dots, s_N\}$) deployed in a target area. The sensing radius of all sensors is assumed to be r . The main objective of the coverage improvement problem is to move sensors to their optimal locations so that the coverage ratio R_c is maximized. Aside from the coverage maximization goal, other objectives could also be considered in deployment improvement such as uniformity of sensors distributed in the monitoring area [37], moving distances of sensor nodes [53], energy consumption optimization [25], [27], and uniform connectivity of sensors [37].

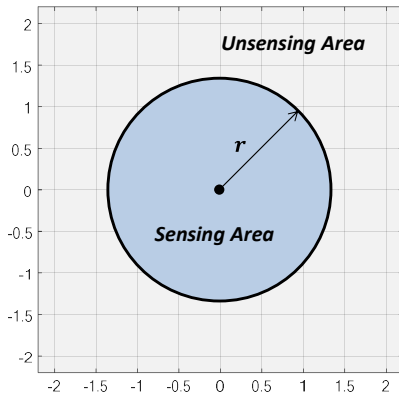


Fig. 1. Binary sensor model.

IV. Virtual Force Algorithm

Zou et al. proposed the Virtual Force Algorithm (VFA) for the redeployment of WSN sensors and coverage maximization [38]. This algorithm is based on intermolecular attractive and repulsive forces. In VFA, virtual forces applied to each sensor are computed based on the relative position of neighboring sensors. The cluster head is responsible for executing the VFA algorithm. It calculates the final position of the sensors in several iterations so that at the end of the algorithm, it has computed the near-optimal sensor positions. Then the sensors move to these calculated positions (one-time movement) which causes them to be placed at an optimal distance from each other [38].

There are two sensor detection models used in WSNs (the binary detection model and the probabilistic model). In the binary model, the probability of detecting an event within the sensing range of the sensor is one, otherwise, the probability is zero. The binary sensor model is shown in Fig. 1. In the probabilistic sensor model, the probability of detecting a target decreases with increasing distance between the target and the sensor. Although the probabilistic model is more compatible with the real world, since the sensor model does not affect how the sensors are positioned in the virtual force algorithm, here, the binary model is considered for the sake of simplicity.

The pseudo-code of the virtual force algorithm is shown in Algorithm A1 [38]. Suppose we have N sensors whose position in a monitoring area should be optimized. In each iteration of the virtual force algorithm, the attractive or repulsive forces between every two sensors are first computed and then the virtual position of each sensor is adjusted based on the total force applied to it. The algorithm stops when the number of iterations reaches M , or no improvement is observed in the coverage rate during L consecutive iterations. Finally, the best placement achieved for sensors is considered the final placement, and the sensors move to new locations by one-time movement. In this pseudocode, running the algorithm for L iterations even if the coverage rate does not change, gives the algorithm enough time to try to exit the local minimums.

```

• Generate grid points for coverage computation
for  $t = 1..M$  do
  • Compute coverage ratio using equation (1)
  if coverage ratio is not improved for  $L$  iterations then
    exit loop
  end
  for  $i = 1..p$  do
    • Compute distance of every sensor to sensor  $s_i$ 
    • Compute virtual force of every sensor applied to sensor  $s_i$ 
      using equation (2)
    • Compute total force applied to sensor  $s_i$  using equation (3)
  end
  for  $i = 1..p$  do
    • Move sensor  $s_i$  to new position using equation (4)
  end
end
• Compute coverage ratio for final deployment

```

Algorithm A1. The traditional virtual force algorithm (VFA) [38] for improving sensor deployment.

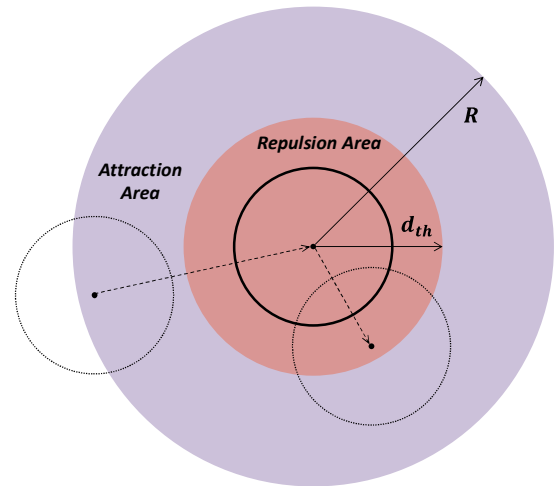


Fig. 2. Attraction area and repulsion area around the sensor in binary sensor model.

In the VFA algorithm, the optimal distance d_{th} is used to control the distance of sensors from each other. The algorithm tries to deploy every two neighboring sensors at the optimal distance from each other. If two neighboring sensors get too close, they must repel each other to avoid concentration in one part of the monitoring area. On the other hand, if a pair of neighboring sensors are far, they absorb each other to ensure that a globally uniform sensor placement is achieved. Non-neighboring sensors do not affect each other. The magnitude and direction of the force exerted on the sensor s_i from sensor s_j are shown by (F_{ij}, θ_{ij}) and are calculated according to the following equation [38]:

$$(F_{ij}, \theta_{ij}) = \begin{cases} (WA(d_{ij} - d_{th}), \alpha_{ij}) & \text{if } d_{th} < d_{ij} < R \\ \left(WR \frac{1}{d_{ij}}, \alpha_{ij} + \pi \right) & \text{if } d_{ij} < d_{th} \\ (0,0) & \text{otherwise} \end{cases} \quad (2)$$

where WA (WR) measures the strength of attractive (repulsive) force, d_{ij} indicates the Euclidian distance between s_i and s_j , and d_{th} is the optimal distance. The parameter R determines the maximum absorption distance between two neighboring

sensors and plays the role of the neighborhood radius, and α_{ij} is the orientation (angle) of a line segment from s_i to s_j .

The attraction and repulsion regions in the binary sensor model are shown in Fig. 2. If the distance between two neighboring sensors is less than the optimal, a repulsive (negative) force is applied between them, whose value is linearly proportional to the inverse of the distance between these two sensors. If the distance between two neighboring sensors is larger than the optimal distance, the attractive (positive) force is applied between them, whose value is linearly proportional to the Euclidian distance of these two sensors. No force is considered between two sensors that are not neighbors.

After calculating the attractive and repulsive forces between sensors, the total force exerted on each sensor should be calculated. To calculate the total force vector applied to each sensor, the sum of the applied force vectors or their average can be used. Our studies showed that when the number of sensors is large, the use of the sum of the force vectors on the sensor recommended by Zou in [38], will lead to significant and intense movements of the sensors and prevents the algorithm from converging to a suitable arrangement. For this reason, for all virtual force-based methods, we used the average of the force vectors on each sensor to calculate the vector of the total force on the sensor. The total force vector is calculated as follows:

$$V_i(t) = \frac{1}{|N_i|} \sum_{j \in N_i} V_{ij} \quad (3)$$

where V_{ij} represents the virtual force exerted on s_i sensor by another sensor s_j . The N_i symbol indicates the neighboring sensor set of s_i .

Then, based on the total force vector and the current position of each sensor, its new position is calculated according to the following equation:

$$X_i(t+1) = X_i(t) + V_i(t) \quad (4)$$

where $X_i(t)$ represents the current position of the s_i , $V_i(t)$ indicates the total force vector on the sensor s_i at the current time, and $X_i(t+1)$ shows the new position of sensor s_i in the next iteration. In Fig. 3, the total force on s_1 from s_2 and s_3 is calculated. Since the distance between s_1 and s_2 is larger than d_{th} , the s_2 exerts an attractive force on s_1 , which is represented by an attractive vector between the two sensors. On the other hand, the distance between s_1 and s_3 is minor than d_{th} , so s_3 repels s_1 . The mean vector of these two virtual force vectors is calculated as the total force exerted on s_1 , shown in Fig. 3 with a thicker arrow.

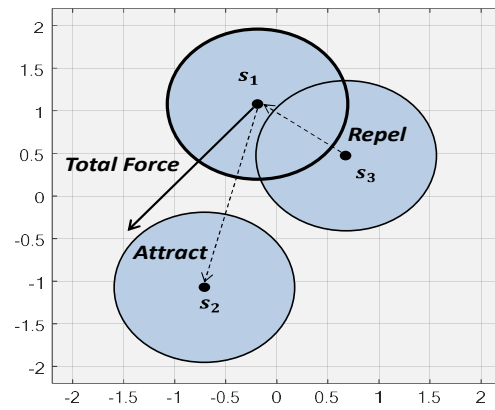


Fig. 3. Attraction and repulsion forces between sensors [38], [44].

V. Improved Virtual Force Algorithm based on the States of Matter

The classical virtual force algorithm is inspired by the motion of matter molecules and the forces of attraction and repulsion between them. However, in the traditional form of the virtual force algorithm, parameter values are fixed during the algorithm's execution. Therefore, the virtual force algorithm (VFA) cannot adapt to the input conditions. The results of previous research show that if the values of the parameters of this algorithm change dynamically over time based on the conditions of the input, the performance of the algorithm will improve in terms of coverage rate. In this section, we propose a dynamic adaptive virtual force algorithm that changes the value of its parameters during execution based on the time, the number of sensors, sensing radius, and size of the monitoring area. Our proposed algorithm is inspired by real-world states of matter. In the real world, matter can be found in three forms: gaseous, liquid, and solid. The molecules in the gas state are volatile and continuously move away from one another. In the liquid state, molecules bind to each other, have cohesion and absorb each other. In the solid state, the molecules adhere entirely to each other and stay almost in place. In this section, an improved virtual force algorithm based on the states of matter (IVFASM) is introduced by considering different states of matter and dynamically adjusting parameter values of the virtual force algorithm over time.

Our proposed IVFASM algorithm in three stages assumes that the matter transitions from the gaseous state to the liquid and then to the solid. This mode change is shown in Fig. 4. First, when the matter is in a gaseous state, sensors strongly escape from each other. Since the sensors are prevented from crossing the border of the monitored area, their escape from each other causes them to be better distributed in the target area, reduces the amount of overlap, and increases the coverage rate dramatically. The gaseous state allows the sensors to be evenly dispersed and cover the entire target area. After that, the

material becomes liquid, and its density gradually increases. As density of molecules increases, the repulsive forces between molecules gradually weaken and attraction's influence increases. In this way, neighboring sensors absorb each other. The small holes formed between the sensors gradually fill during the liquid state, resulting in a uniform coverage. In the last stage, it is assumed that the density of the molecules and the attraction impact have increased to such an extent that the liquid has solidified. In this situation, the movement of sensors is restricted to a small range around them, and the sensors attempt to stabilize their final location by examining their neighbors.

A critical parameter of VFA is the optimal distance between sensors which strongly affects the coverage of final deployment. Our proposed IVFASM algorithm first computes a proper value for optimal distance based on the input conditions. After that, IVFASM dynamically adjusts the value of some other parameters that affect the strength of virtual forces between sensors over time. The pseudo-code of the proposed IVFASM algorithm is described in Algorithm A2. First of all, the value of the optimal distance parameter is computed by IVFASM by considering the number of sensors, sensing radius, and size of the monitoring area. Then, in several iterations, the deployment of sensors is improved. In each iteration, the kinetic energy of matter molecules, the value of repulsion coefficient, and the value of attraction radius are updated according to the current state of matter. Then, virtual forces between sensors are computed and the position of sensors is modified. In this section, details of the proposed method will be described.

A. Determining the Optimal Distance

The optimal distance is a critical parameter of the virtual force algorithm, and its incorrect adjustment will result in limited coverage in the final placement. In [38] authors suggested the user select a proper value for optimal distance manually by running the algorithm several times and plotting the convergence rate versus optimal distance for each sample problem. This is a time-consuming process and may be error-prone. On the other hand, using a constant value of optimal distance for all input problems would lead to poor coverage results. Thus, we suggest choosing the optimal distance automatically and adaptively. When covering a wide area with a small number of sensors, the optimal distance should be large to avoid overlapping. When the number of sensors is high, on the other hand, the algorithm should allow the sensors to overlap so that small gaps between them are also covered. As a result, the number of sensors can be used to determine the proper value for optimal distance. A rational range can be used to choose the best optimal distance value.

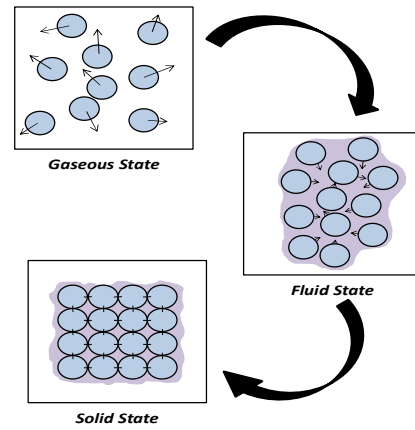
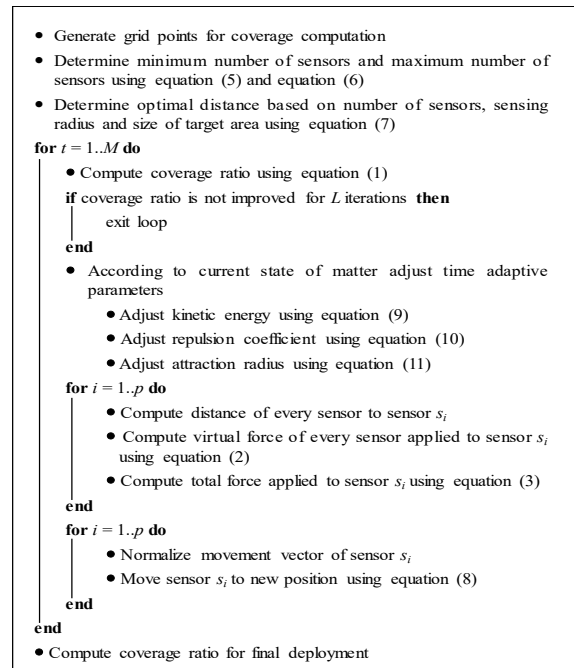


Fig. 4. The behavior of molecules in different states of matter.



Algorithm A2. The pseudo-code of the proposed improved virtual force algorithm based on the states of matter (IVFASM) for improving sensor deployment.

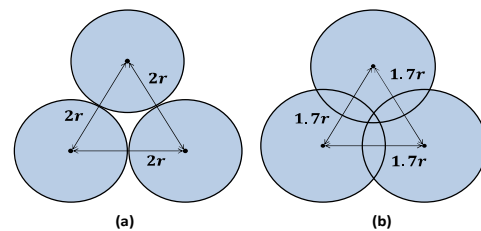


Fig. 5. The role of optimal distance in locating sensors [38], [44]: (a) sensors without overlap, (b) sensors with overlap.

To obtain a relationship between optimal distance and the number of sensors, suppose the entire rectangular region should be covered with a proper number of sensors. If the overlap between sensors is not allowed, the optimal distance

should be set to $d_{th}=2r$, as Fig. 5 (a). In this case, counting the number of squares with side length $2r$ that cover the entire target area yields the appropriate number of sensors, similar to Fig. 6. As a result, the minimum number of sensors needed to cover the entire rectangular region can be estimated by dividing the target rectangle's area by the area of a square with a side length of $2r$, as follows:

$$p_{min} = \left\lceil \frac{(x_{max}-x_{min}) \cdot (y_{max}-y_{min})}{4r^2} \right\rceil \quad (5)$$

where, the target area is assumed to be a rectangle in the range $[x_{min},x_{max}] \times [y_{min},y_{max}]$. If the number of sensors is less than or equal to p_{min} , the optimal distance should be set to $d_{th}=2r$ to prevent overlap.

When a high number of sensors is available, the algorithm should allow them to overlap to increase coverage and fill gaps by setting the optimal distance to a value less than $2r$, as shown in Fig. 5 (b). In this case, setting the optimal distance equal to $d_{th}=\sqrt{3}r$ is sufficient to achieve maximum coverage across the rectangular target area [53]. In this paper, to estimate the minimum number of sensors needed to fully cover the entire target area while overlap is allowed, it is assumed that, similar to Fig. 7, the target area is virtually divided into several regular hexagons with side-length r and each hexagon has a sensor placed on the hexagon center. The minimum number of sensors needed to fully cover the target area, according to the deployment shown in Fig. 7, is:

$$p_{max} = \left\lceil \frac{(x_{max}-x_{min})}{1.5r} \right\rceil * \left(\left\lceil \frac{(y_{max}-y_{min})}{\sqrt{3}r} \right\rceil + 0.5 \right) \quad (6)$$

Thus, the optimal distance may be set to $d_{th}=\sqrt{3}r$, if the number of sensors is equal to or larger than p_{max} .

In IVFASM, the relation $d_{th}=\beta \cdot r$ is used to determine the value of optimal distance adaptively. If the number of sensors equals p_{min} or less, the coefficient β is set to $\beta_{max}=2$. If the number of sensors equals p_{max} or more, the coefficient β is set to $\beta_{min}=\sqrt{3}$. If the number of sensors is between p_{min} and p_{max} , IVFASM approximates the appropriate value for coefficient β in the range $\sqrt{3} < \beta < 2$ by a linear relation as follows:

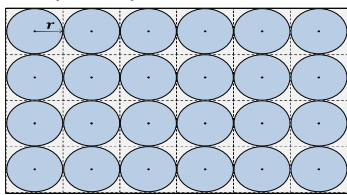


Fig. 6. Coverage of the entire target area without overlap between sensors.

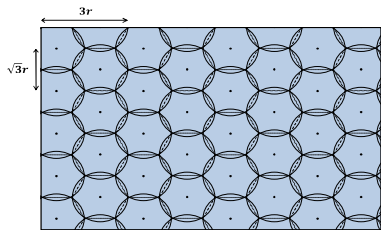


Fig. 7. Coverage of the entire target area with overlap between

sensors and optimal distance of $\sqrt{3}r$ [53].

$$\beta = \beta_{max} - (\beta_{max} - \beta_{min}) \left(\frac{p-p_{min}}{p_{max}-p_{min}} \right) \quad (7)$$

In this relation, as the number of sensors p increases, the optimal distance decreases to take advantage of the ability provided by more sensors to fill the gaps in the field.

B. Simulating the States of Matter

An optimal arrangement of sensors should cover the entire target area, not have holes, and distribute sensors uniformly throughout the monitoring area. Such an arrangement should make the most of the capability of existing sensors. For this reason, in our method, sensors are considered matter molecules. It is assumed that the matter is first in the gaseous state, then in liquid, and then in solid. The density of matter steadily increases while the strength of molecule motion decreases during this transition process. Over time, molecules steadily absorb each other more and escape each other less. To realize the states of matter in the virtual force algorithm, the concept of the kinetic energy of the molecules is considered in the proposed method, and the strength of repulsion forces between the molecules and their attraction radius is adjusted according to different states of matter.

The state of matter is divided into three time-stages: gas, liquid, and solid. If the start time of the liquid state is denoted by ts_{fluid} and its end time is denoted by tf_{fluid} , the material is in the gaseous state before the ts_{fluid} and in the solid state after the tf_{fluid} , and in the liquid state between the two times.

C. Adjustment of Kinetic Energy

To incorporate the kinetic energy of matter molecules into the virtual force algorithm, in this paper we normalize the movement vector of each sensor and dynamically modify its size based on the kinetic energy of matter molecules. Assume that V'_i represents normalized movement vector of sensor s_i , and X_i shows the current position of sensor s_i . In IVFASM, the location of every sensor s_i is changed in every iteration as:

$$X_i(t+1) = X_i(t) + \rho(t)V'_i(t) \quad (8)$$

where $\rho(t)$ indicates the kinetic energy coefficient of matter, and t shows the iteration number.

The level of kinetic energy coefficient must be determined dynamically over time based on the state of matter. The maximum value of $\rho(t)$ indicates the maximum amount of sensor displacement in every iteration. Suppose show maximum displacement value with ρ_{max} and minimum displacement value with ρ_{min} . The value of the kinetic energy coefficient should be determined between these two values in each iteration. In the gas state, IVFASM considers the kinetic energy to be maximal and constant as ρ_{max} . In the solid state, IVFASM considers the kinetic energy constant and equal to its minimum value ρ_{min} . In the liquid state, the density of the liquid increases progressively, and therefore the amount of kinetic energy is reduced in IVFASM from maximum to minimum as:

$$\rho(t) = \rho_{max} - \left(\frac{t-t_{sfluid}}{t_{ffluid}-t_{sfluid}} \right) (\rho_{max} - \rho_{min}) \quad (9)$$

D. Adjustment of Repulsion Coefficient

When the matter is in the gaseous state, the molecules intensely repel each other. In the liquid state, the repulsion between molecules is reduced. In the solid state, there is almost no repulsion. On the other hand, due to the normalization of the virtual force vector in the proposed method, only the relative magnitudes of attraction and repulsion to each other are important, and the magnitude of each value independently does not affect the outcome. Accordingly, in IVFASM, the value of attraction coefficient WA is set to a constant value, and the value of the repulsion coefficient WR is adjusted over time depending on the state of matter. When the matter is in the gaseous state, the repulsion coefficient is set to WR_{max} , and when the matter is in the solid state, the repulsion coefficient is set to WR_{min} . In the liquid state, the value of the repulsion coefficient is reduced gradually according to the following equation:

$$WR(t) = WR_{max} - \left(\frac{t-t_{sfluid}}{t_{ffluid}-t_{sfluid}} \right) (WR_{max} - WR_{min}) \quad (10)$$

E. Adjustment of Attraction Radius

In the virtual force algorithm, the attraction radius represents the maximum distance between two neighboring sensors. If two neighbors are located at a distance between d_{th} to R , the attraction will be applied between them. Since molecules cannot absorb each other in the gaseous state, one may conclude that their attraction radius is minimal. In IVFASM, the attraction radius of the sensors is gradually increased as the state of matter changes to a liquid and then a solid. In the gas state, the attraction radius is set to R_{min} and in the solid state to R_{max} . In the liquid state, the attraction radius is increased over time as:

$$R(t) = R_{min} + \left(\frac{t-t_{sfluid}}{t_{ffluid}-t_{sfluid}} \right) (R_{max} - R_{min}) \quad (11)$$

VI. Experimental Results

To verify the effectiveness of the IVFASM algorithm, it is implemented in MATLAB 2021b and executed on a computer system with an Intel Core 2 Duo P8700 2.53 GHz processor and 4.00 GB of main memory. Performance of the algorithm is evaluated by coverage ratio, non-uniformity, computation time, and compared with genetic algorithm (GA), particle swarm optimization (PSO), fuzzy redeployment algorithm (FRED) [54], classical virtual force algorithm (VFA) [38], and improved virtual force based on area intensity (IVFAI) [44] all implemented in MATLAB 2021b.

A. Experimental Setup

To compare algorithms, it is assumed that the different number of sensors with two values of sensing radius $r=0.3$ and $r=0.4$ are initially randomly distributed in a monitoring area with dimensions $[-2,+ 2] \times [-2,+ 2]$, and the deployment of sensors is improved by each algorithm. All algorithms are

applied to the same initial conditions to make the comparisons fair.

In the genetic algorithm (GA), each chromosome is a sequence of pairs (dx_i, dy_i) that shows the displacement of the sensor s_i relative to its initial position. One-point crossover operator is used to combining individuals. In the mutation operator, one of the sensors is randomly selected and its position is shifted by two random values in the range $[-r/2, +r/2]$ in horizontal and vertical directions. In our implementation of GA, population size is set to 50 individuals, crossover rate is set to 0.70, and mutation rate is set to 0.1. A similar approach was already proposed in [55].

In particle swarm optimization (PSO), the representation of particles is considered similar to the representation of individuals in GA. In PSO movement of each particle is influenced by the global best position, and the personal best position, updated as better positions are found over time. In our experiments, a population of 50 particles, inertia weight of 0.04, social learning weight of 0.1, cognitive learning weight of 0.1, and mutation probability of 0.1 are used when running the PSO algorithm.

TABLE 2
SIMULATION PARAMETER SETTINGS FOR IVFASM

Parameter	Symbol	Value
Maximum iterations	M	100
Convergence iterations	L	15
Start time of fluid state	t_{sfluid}	20
End time of fluid state	t_{ffluid}	80
Max optimal distance coeff	β_{max}	2
Min optimal distance coeff	β_{min}	$\sqrt{3}$
Maximum kinetic energy	ρ_{max}	$0.20r$
Minimum kinetic energy	ρ_{min}	$0.01r$
Attraction coefficient	WA	0.01
Maximum repulsion coefficient	WR_{max}	0.20
Minimum repulsion coefficient	WR_{min}	0.05
Maximum attraction radius	R_{max}	$3r$
Minimum attraction radius	R_{min}	r

FRED uses the Voronoi diagram to determine the optimal position of sensors and a fuzzy system to decide whether each sensor should move or not [54]. Sensors are moved step by step toward their optimal locations by FRED in several iterations. In our experiments, parameters of the FRED method are set to $\beta=2$ and neighborhood radius $R_c=3r$.

In the classical virtual force algorithm (VFA) [38], the attraction coefficient is set to $WA=0.01$, the repulsion coefficient is set to $WR=0.1$, and the absorption radius is set to $R=3r$.

In the improved virtual force algorithm based on area intensity (IVFAI) [44], the optimal distance of each sensor is determined based on the intensity of neighbors in the sensor's

local neighborhood. IVFAI's objective is to make the density of sensors uniform throughout the monitoring area. When the area intensity of the current sensor is higher than average, its optimal distance is set to $2r$, otherwise, it is set to $\sqrt{3}r$. In our experiments, $WR=0.1$, $WA=0.01$, and $R=3r$ are used for IVFAI.

B. Parameter Setting

The maximum number of iterations in each algorithm is set to $M=100$. For all algorithms evaluated, the convergence criterion is defined as the change in the coverage ratio in the last $L=15$ iterations. This number of iterations was found to be an adequate number of iterations for convergence to take place. Simulation parameters of the proposed method IVFASM are set according to Table II. In our experiments, most iterations of the IVFASM are assigned to the liquid state so that the proposed algorithm has sufficient time to gradually modify the location of the sensors by considering both repulsive and attractive forces. Accordingly, the start time of the fluid state is set to $ts_{fluid}=20$ and its end time is set to $tf_{fluid}=80$. The optimal distance of the sensors is selected from the range of no hole between sensors with $\beta_{min}=\sqrt{3}$ to no overlap between sensors with $\beta_{max}=2$. The value of kinetic energy of sensors is considered a fraction of the sensing radius to gradually move sensors in small steps to their optimal locations over time. Thus, minimum kinetic energy is set to $\rho_{min}=0.01r$ and maximum kinetic energy is set to $\rho_{max}=0.20r$. Since sensors have a high overlap in their initial deployment, the repulsion of sensors is more important than their attraction. The coefficient of the repulsive force in IVFASM is accordingly set to a higher value than the coefficient of attractive force $WA=0.01$, and gradually changed from $WR_{max}=0.20$ to $WR_{min}=0.05$ in the liquid state of matter. The minimum attraction radius is set to $R_{min}=r$ because overlapped sensors should repel each other instead of attracting. On the other hand, the maximum attraction radius is set to $R_{max}=3r$ so that neighboring sensors can support and absorb each other to provide uniform coverage of the monitoring area.

C. The Role of States of Matter

Considering the states of matter in the proposed method causes a more uniform distribution of sensors in the target area and a significant increase in coverage rate. In the proposed IVFASM algorithm, the matter is considered in three states gas, liquid, and solid. Deployment of the sensors at the end of each time stage is visualized in Fig. 8 for 30 sensors with a sensing radius of $r=0.4$. In the gas state, IVFASM reduces the overlapping of sensors very quickly and distributes sensors throughout the target area by adjusting the strength of repulsive forces on high values and escaping sensors from each other. This caused the sensors to expand rapidly in the monitoring area and increased the coverage ratio dramatically as shown in Fig. 8 (b) compared to the initial deployment in Fig. 8 (a). In the liquid state, IVFASM moves sensors more slowly and gradually propels them to their optimal locations by enabling sensors both absorb and repel each other to approach equilibrium. As a result, in Fig. 8 (c) sensors provide more uniform coverage of the monitoring area compared with Fig. 8 (b). In the last stage, at solid state, IVFASM moves sensors very little and searches the local neighborhood of each sensor for a better place. Accordingly, in Fig. 8 (d) sensors are placed in their final optimal place.

The trend of coverage improvement in the proposed IVASM algorithm is visualized by a plot in Fig. 9. Since the kinetic energy of the molecules is high in the gas state, and the repulsive forces are strong, overlapping sensors would repel each other with great power. This has caused a sharp increase in the coverage ratio in the left part of Fig. 9. In the liquid state, sensors search their neighborhood for a better place, which causes oscillations in coverage ratio as the liquid state starts, seen in the middle part of Fig. 9. These oscillations originate primarily from the displacement of each sensor between the gravitational zone and the repulsive zone of its neighboring sensors and will continue as long as the sensors are not optimally spaced relative to each other.

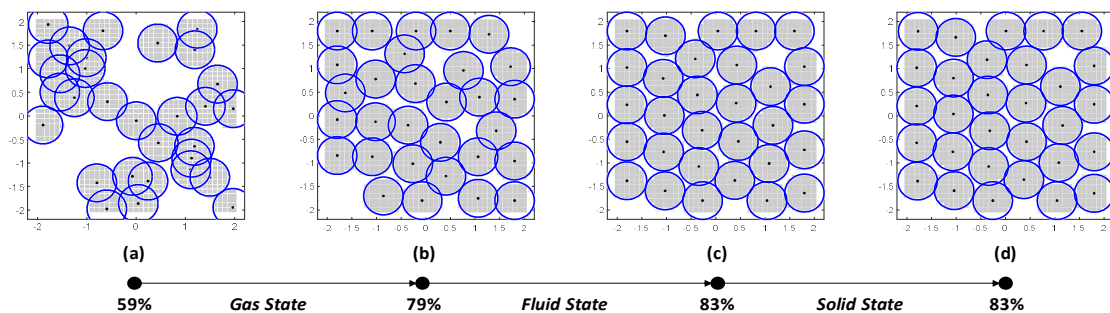


Fig. 8. The improvement of sensor placement overtime at different states of matter by IVFASM for 30 sensors with perception radius $r=0.4$.

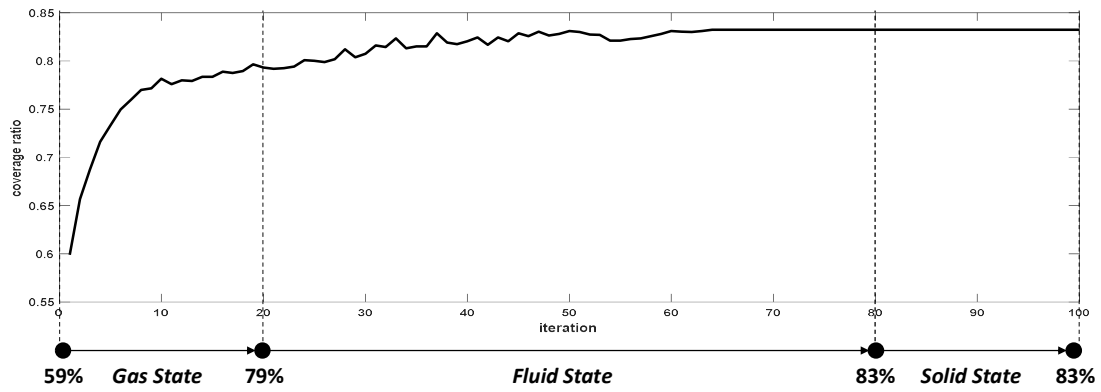


Fig. 9. The trend of coverage ratio improvement at different states of matter by IVFASM for 30 sensors with perception radius $r=0.4$.

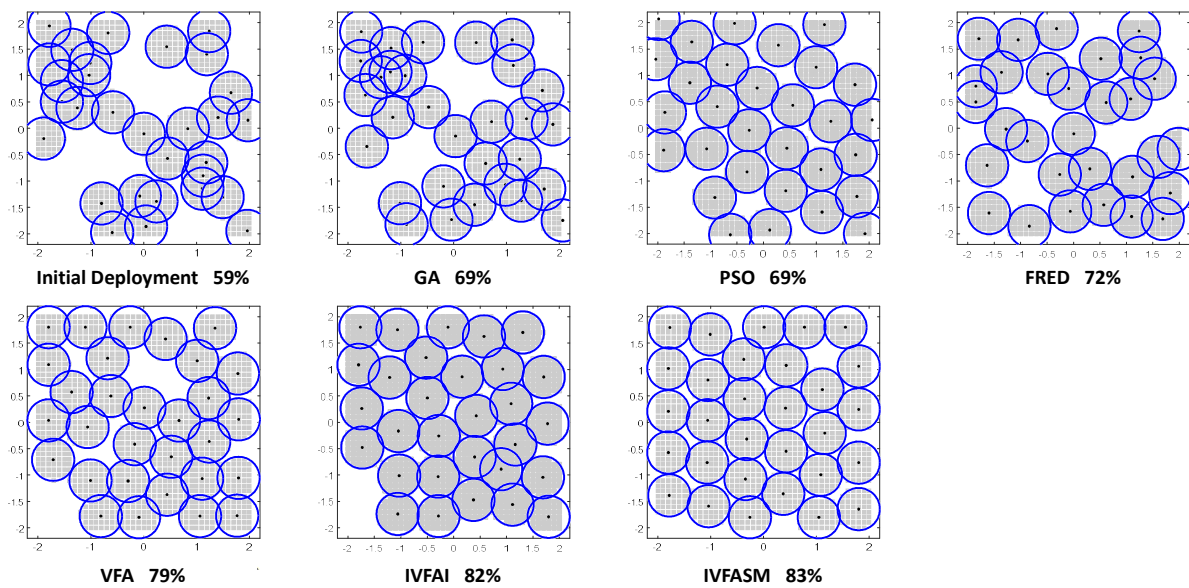


Fig. 10. The improvement of sensor placement by various algorithms for 30 sensors with perception radius $r=0.4$.

In our proposed IVFASM method, the value of several parameters changes over time, gradually reducing the magnitude of these fluctuations and also helping the proposed algorithm to escape the local minimum. As a result, as time goes, the strength of these oscillations decreased in Fig. 9. In general, the overall trend of coverage ratio has been upward in this time stage. In the solid state, the kinetic energy of sensors is very low, and their repulsive forces are very weak, which causes the sensors strongly absorb each other in their final location like molecules of a solid. As a result, the coverage ratio would not change significantly in the solid state, as observed no change in the right part of Fig. 9.

D. Coverage Improvement

The main objective of WSN redeployment algorithms is to improve the coverage quality of the mobile sensor network. The quality of the final deployment generated by the proposed IVFASM algorithm is compared visually with other

algorithms in Fig. 10. For each algorithm, the coverage ratio of the resulted deployment is also written next to the name of the algorithm. The proposed IVFASM algorithm produced a uniform deployment of sensors that covers most regions of the monitoring area and has provided the most significant increase in coverage ratio to 83% among evaluated algorithms. In contrast, the GA method has not been successful in distributing sensors evenly throughout the target area, and many sensors still significantly overlap. GA achieved a coverage ratio of 69%. PSO deployed sensors better than GA and reduced overlap between sensors, but some regions of the target area are not covered at all and many holes exist between sensors. This has caused the coverage ratio of PSO to be similar to the GA of 69%. FRED method made some overlap between neighboring sensors to avoid holes between them and obtained a bit better coverage ratio of 72%. Virtual-force-based algorithms VFA, IVFAI, and IVFASM distributed sensors uniformly in the monitoring area and obtained coverage ratios

of 79%, 82%, and 83%, respectively. The proposed method IVFASM produced the best deployment by covering all regions of the target area uniformly.

The coverage ratio is the most important quality metric in the evaluation of sensors redeployment algorithms. To evaluate the coverage quality of final deployments quantitatively, the coverage ratio of produced arrangements is evaluated and summarized in Table III for the different number of sensors and two values of sensing radius $r=0.4$ and $r=0.3$. Under the same initial conditions, IVFASM has provided a better coverage ratio than the GA, PSO, FRED, VFA, and IVFAI in most sample problems. For each sample problem in Table III, the performance of the best method is highlighted in blue color, and the performance of the second-best method is differentiated from other methods by boldface. IVFASM has achieved the best or second-best coverage ratio in almost all sample problems in Table III.

TABLE 3

INVESTIGATION OF THE EFFECT OF THE NUMBER OF SENSORS (p) AND PERCEPTION RADIUS (R) ON THE COVERAGE IMPROVEMENT IN EVALUATED ALGORITHMS

r	p	Initial	GA	PSO	FRED	VFA	IVFAI	IVFASM
0.4	10	24.15	29.12	30.81	29.80	29.21	29.74	29.92
	20	38.37	48.19	52.35	52.77	54.13	57.35	58.12
	30	59.90	69.01	69.19	72.34	79.30	82.63	83.22
	40	65.68	76.15	79.24	79.83	93.99	92.68	95.78
	50	76.86	85.90	84.53	87.39	99.58	98.45	99.70
	60	83.82	91.43	92.03	91.08	100	99.70	100
	70	87.03	94.88	95.48	96.91	99.88	100	100
0.3	10	15.05	17.73	18.38	16.89	16.95	17.13	17.25
	20	25.34	31.65	31.77	31.23	32.42	33.31	33.37
	30	40.93	45.27	47.06	46.46	47.89	49.02	50.68
	40	45.87	53.48	55.09	60.92	63.77	65.20	66.39
	50	58.18	64.49	65.14	72.40	77.81	79.83	79.00
	60	66.33	70.97	74.00	80.55	88.82	90.84	91.73
	70	70.79	78.94	75.73	84.71	96.85	95.95	97.68

When the number of sensors is very small, scattered but non-uniform distribution can lead to a higher coverage ratio than a uniform distribution. In addition, when the number of sensors is very small, the result of virtual force-based algorithms depends highly on the initial location of the sensors, their proximity to the boundary of the target area, and their initial distance from each other. For the case of 10 sensors, for example, the PSO algorithm in Table III has achieved a higher coverage rate than our proposed method due to the freedom in changing position of sensors and the lack of virtual forces between neighboring sensors. However, with the increase in the number of sensors, the virtual forces between the sensors have helped to distribute them evenly in the target area, and our proposed method has achieved better results than PSO.

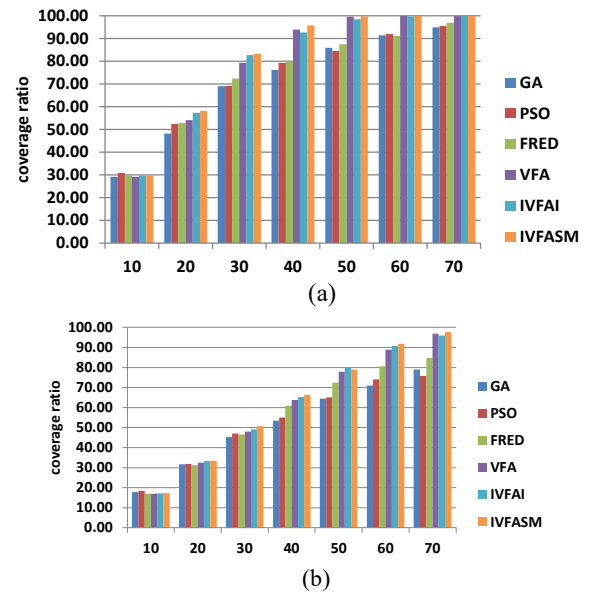


Fig. 11. Coverage ratio with the number of sensors in various algorithms for (a) detection radius $r=0.4$, (b) detection radius $r=0.3$.

The relationship between coverage ratio and the number of sensors is plotted in Fig. 11 for two values of sensing radius $r=0.4$ and $r=0.3$. In both diagrams, the trend of changes in coverage ratio has always been upward with the increase in the number of sensors. In addition, IVFASM has provided the best coverage ratio for almost every number of sensors, and virtual-force based methods performed much better than GA, PSO, and FRED.

E. Computation Time

Virtual-force-based algorithms are often very fast due to evolving only one solution over time. In contrast, population-based metaheuristics like GA and PSO are computationally intensive because in each iteration they should perform several randomized operations on all individuals in the population. Accordingly, as shown in Fig. 12 virtual-force-based algorithms VFA, IVFAI, and IVFASM are surprisingly multiple times faster than PSO and GA when relocating 30 sensors. To be more precise, GA has taken 32.28 seconds, PSO has taken 40.67 seconds, and IVFASM took only 1.36 seconds for improving the deployment of 30 sensors. The computation time of all evaluated algorithms for the different number of sensors and two values of sensing radius is summarized in Table IV. Results reveal that the virtual-force-based algorithms are at least ten times faster than GA, PSO, and FRED for all sample problems. In this experiment, the time difference between virtual-force-based methods has not been significant.

F. Uniformity of Sensor Deployments

In addition to the coverage ratio, a suitable sensors redeployment algorithm should cover all points of the target area uniformly. To evaluate uniform coverage of the

monitoring area, the uniformity of sensors arrangement could be analyzed. If the distance of each sensor from its k neighboring sensors is calculated, the average standard deviation of neighbor distances indicates the non-uniformity of sensor distribution. Accordingly, the deployment non-uniformity indicator, NU , is calculated as [37]:

$$NU = \frac{1}{N} \sum_{i=1}^N \sigma_i \quad (12)$$

$$\sigma_i = \left(\frac{1}{k} \sum_{j \in N_i} (d_{ij} - M_i)^2 \right)^{\frac{1}{2}} \quad (13)$$

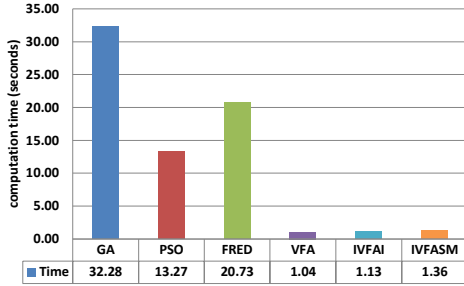


Fig. 12. The computation time of various algorithms for improving the deployment of 30 sensors.

TABLE 4
INVESTIGATION OF THE EFFECT OF THE NUMBER OF SENSORS (p)
AND PERCEPTION RADIUS (r) ON THE COMPUTATION TIME
(SECONDS) OF EVALUATED ALGORITHMS

r	p	GA	PSO	FRED	VFA	IVFAI	IVFASM
0.4	10	18.43	32.06	23.05	0.40	0.87	0.46
	20	30.38	33.71	20.90	0.77	1.23	1.05
	30	32.28	13.27	20.73	1.04	1.54	1.36
	40	32.45	33.73	39.49	1.18	1.01	1.23
	50	32.66	34.18	24.57	1.27	1.10	0.75
	60	33.30	34.12	28.17	0.92	1.33	0.52
	70	34.92	35.38	30.69	1.07	1.18	0.27
0.3	10	29.52	32.51	13.69	0.33	0.79	0.78
	20	30.47	29.56	20.04	0.42	0.88	0.78
	30	29.23	31.63	19.91	0.43	0.81	1.06
	40	32.34	32.91	32.43	0.90	0.95	1.18
	50	33.04	33.95	30.37	0.91	1.37	0.81
	60	16.64	36.10	35.57	0.86	1.33	1.72
	70	36.72	36.71	31.45	1.11	1.13	1.26

where k shows the number of neighboring sensors (here we set $k=5$), N_i represents the set of neighboring sensors of sensor s_i , d_{ij} is the Euclidian distance between adjacent sensor s_i and sensor s_j , and M_i is the average distance between the sensor s_i and all its neighboring sensors.

To evaluate the performance of IVFASM in terms of deployment uniformity, NU is computed for improved output arrangement for the different number of sensors and two sensing radiuses. Results in terms of non-uniformity are summarized in Table V. It can be seen that the proposed IVFASM algorithm provides more uniform deployment than GA and FRED in all sample problems. It also provided more

uniform deployment than VFA, IVFAI, and PSO in most sample problems. Non-uniformity of generated deployment for various algorithms is visualized by radar diagrams in Fig. 13. In general, IVFASM has provided satisfactory uniformity and a higher coverage ratio.

TABLE 5

INVESTIGATION OF THE EFFECT OF THE NUMBER OF SENSORS (p)
AND PERCEPTION RADIUS (r) ON THE NON-UNIFORMITY OF FINAL
DEPLOYMENT IN EVALUATED ALGORITHMS

r	p	GA	PSO	FRED	VFA	IVFAI	IVFASM
0.4	10	0.37	0.32	0.58	0.38	0.38	0.33
	20	0.34	0.29	0.30	0.28	0.23	0.21
	30	0.22	0.25	0.24	0.19	0.16	0.16
	40	0.18	0.17	0.20	0.13	0.16	0.14
	50	0.17	0.19	0.15	0.12	0.16	0.13
	60	0.16	0.18	0.16	0.15	0.15	0.14
	70	0.15	0.16	0.15	0.15	0.13	0.15
0.3	10	0.36	0.38	0.47	0.37	0.37	0.30
	20	0.36	0.37	0.35	0.34	0.34	0.30
	30	0.25	0.24	0.24	0.24	0.23	0.20
	40	0.18	0.18	0.19	0.15	0.13	0.13
	50	0.16	0.15	0.15	0.13	0.10	0.12
	60	0.15	0.16	0.15	0.10	0.10	0.09
	70	0.14	0.15	0.14	0.08	0.11	0.09

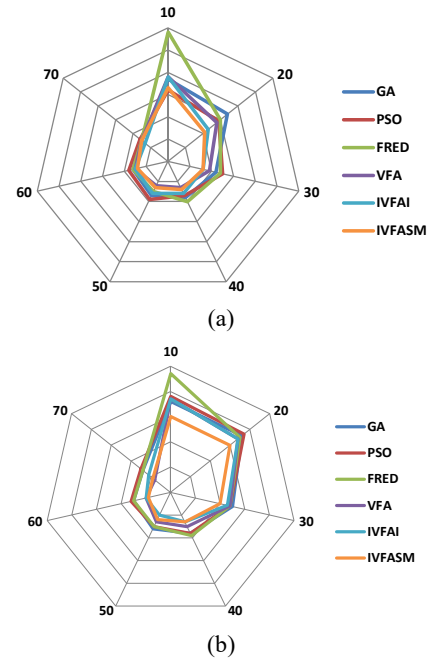


Fig. 13. Non-uniformity (NU) of final deployment with the number of sensors in various algorithms for (a) detection radius $r=0.4$, (b) detection radius $r=0.3$.

VII. CONCLUSIONS

In this paper, considering states of matter, an improved virtual force algorithm IVFASM is proposed that simulates the behavior of molecules in different states of matter to improve the coverage of a mobile wireless sensor network. In our

method, matter transitions from a gaseous state to a liquid to a solid. The position of the sensors is modified by modeling them as matter molecules and applying the forces of attraction and repulsion between them. In the gas state, the kinetic energy of the molecules was considered high and the repulsive force was considered strong. In the liquid state, the strength of the repulsive force gradually decreased with the increasing attraction radius of sensors. In the solid state, low kinetic energy and low repulsive force were applied, while the attraction radius is set to its maximum value. In addition to simulating states of matter, at the beginning of IVFASM, the value of the optimal distance of sensors is adaptively determined based on the number of sensors, their radius, and the size of the target monitoring area. Compared with five other algorithms, the IVFASM method achieved a better arrangement of sensors that covers the target area uniformly and also has a higher coverage ratio. Extension of the states of matter to other issues in sensor network design could be the subject of future research works.

REFERENCES

- [1] S. M. Mohamed, H. S. Hamza, and I. A. Saroit, "Coverage in mobile wireless sensor networks (M-WSN): A survey," *Comput. Commun.*, vol. 110, pp. 133–150, Sep. 2017, doi: 10.1016/j.comcom.2017.06.010.
- [2] M. Farsi, M. A. Elhosseini, M. Badawy, H. Arafat Ali, and H. Zain Eldin, "Deployment techniques in wireless sensor networks, coverage and connectivity: A survey," *IEEE Access*, vol. 7, pp. 28940–28954, Feb. 2019, doi: 10.1109/ACCESS.2019.2902072.
- [3] M. Younis and K. Akkaya, "Strategies and techniques for node placement in wireless sensor networks: A survey," *Ad Hoc Netw.*, vol. 6, no. 4, pp. 621–655, Jun. 2008, doi: 10.1016/j.adhoc.2007.05.003.
- [4] S. S. S. Farahani and S. Fakhimi Derakhshan, "LMI-based congestion control algorithms for a delayed network," *International Journal of Industrial Electronics Control and Optimization*, vol. 2, no. 2, pp. 91–98, Apr. 2019, doi: 10.22111/ieco.2018.24948.1038.
- [5] M. N. Ismail, M. A. Shukran, M. R. M. Isa, M. Adib, and O. Zakaria, "Establishing a soldier wireless sensor network (WSN) communication for military operation monitoring," *Int. J. Inf. Commun. Technol.*, vol. 7, no. 2, pp. 89–95, Aug. 2018, doi: 10.11591/ijict.v7i2.pp89-95.
- [6] B. Prabhu, M. Pradeep, and E. Gajendran, "Military applications of wireless sensor network system," *A Multidisciplinary Journal of Scientific Research & Education*, vol. 2, no. 12, Dec. 2016. Available: <https://papers.ssrn.com/abstract=2905627>.
- [7] Y. Yang, Z. Bai, Z. Hu, Z. Zheng, K. Bian, and L. Song, "AQNet: Fine-grained 3D spatio-temporal air quality monitoring by aerial-ground WSN," in *IEEE Conference on Computer Communications Workshops*, pp. 1–2, 2018. doi: 10.1109/INFCOMW.2018.8406985.
- [8] D. Shinde and N. Siddiqui, "IOT based environment change monitoring & controlling in greenhouse using WSN," in *International Conference on Information, Communication, Engineering and Technology (ICICET)*, pp. 1–5, 2018. doi: 10.1109/ICICET.2018.8533808.
- [9] J. Aponte-Luis, J. A. Gómez-Galán, F. Gómez-Bravo, M. Sánchez-Raya, J. Alcina-Espigado, and P. M. Teixido-Rovira, "An efficient wireless sensor network for industrial monitoring and control," *Sensors*, vol. 18, no. 1, Art. no. 182, Jan. 2018, doi: 10.3390/s18010182.
- [10] J. Jiang, H. Wang, X. Mu, and S. Guan, "Logistics industry monitoring system based on wireless sensor network platform," *Comput. Commun.*, vol. 155, pp. 58–65, Apr. 2020, doi: 10.1016/j.comcom.2020.03.016.
- [11] M. Y. Aalsalem, W. Z. Khan, W. Gharibi, M. K. Khan, and Q. Arshad, "Wireless sensor networks in oil and gas industry: Recent advances, taxonomy, requirements, and open challenges," *J. Netw. Comput. Appl.*, vol. 113, pp. 87–97, Jul. 2018, doi: 10.1016/j.jnca.2018.04.004.
- [12] L. García et al., "Deployment strategies of soil monitoring WSN for precision agriculture irrigation scheduling in rural areas," *Sensors*, vol. 21, no. 5, Art. no. 1693, Jan. 2021, doi: 10.3390/s21051693.
- [13] Wajiran, S. D. Riskiono, P. Prasetyawan, A. Mulyanto, M. Iqbal, and R. Prabowo, "Control and realtime monitoring system for mushroom cultivation fields based on WSN and IoT," *J. Phys.: Conf. Ser.*, vol. 1655, no. 1, Art no. 012003, Oct. 2020, doi: 10.1088/1742-6596/1655/1/012003.
- [14] J. G. Caicedo-Ortiz et al., "Monitoring system for agronomic variables based in WSN technology on cassava crops," *Comput. Electron. Agric.*, vol. 145, pp. 275–281, Feb. 2018, doi: 10.1016/j.compag.2018.01.004.
- [15] S. K.M. and S. R. M.S., "IoT and WSN based water quality monitoring system," in *3rd International conference on Electronics, Communication and Aerospace Technology (ICECA)*, pp. 205–210, 2019. doi: 10.1109/ICECA.2019.8821859.
- [16] P. Soni, A. K. Pal, and S. H. Islam, "An improved three-factor authentication scheme for patient monitoring using WSN in remote health-care system," *Comput. Methods Programs Biomed.*, vol. 182, Art no. 105054, Dec. 2019, doi: 10.1016/j.cmpb.2019.105054.
- [17] G. Baig Mohammad and S. Shitharth, "Wireless sensor network and IoT based systems for healthcare application," *Materials Today: Proceedings*, Mar. 2021, doi: 10.1016/j.matpr.2020.11.801.
- [18] A. Liu and S. Zhao, "High-performance target tracking scheme with low prediction precision requirement in WSNs," *Int. J. Ad Hoc Ubiquitous Comput.*, vol. 29, no. 4, pp. 270–289, Jan. 2018, doi: 10.1504/IJAHUC.2018.096081.
- [19] J. R. Parvin and C. Vasanthanayaki, "Particle swarm optimization-based energy efficient target tracking in wireless sensor network," *Measurement*, vol. 147, Art no. 106882, Dec. 2019, doi: 10.1016/j.measurement.2019.106882.
- [20] J. Luo, Z. Zhang, C. Liu, and H. Luo, "Reliable and cooperative target tracking based on WSN and WiFi in indoor wireless networks," *IEEE Access*, vol. 6, pp. 24846–24855, 2018, doi: 10.1109/ACCESS.2018.2830762.
- [21] M. A. Khan, M. A. Khan, M. Driss, W. Boulila, and J. Ahmad, "Evolution of target localization in wireless sensor network (WSN): A review," in *International Congress of Advanced Technology and Engineering (ICOTEN)*, pp. 1–8, 2021. doi: 10.1109/ICOTEN52080.2021.9493510.
- [22] M. A. U. Rehman, R. Ullah, B.-S. Kim, B. Nour, and S. Mastorakis, "CCIC-WSN: An architecture for single-channel cluster-Based information-centric wireless sensor networks," *IEEE Internet Things J.*, vol. 8, no. 9, pp. 7661–7675, May 2021, doi: 10.1109/JIOT.2020.3041096.
- [23] P. Maheshwari, A. K. Sharma, and K. Verma, "Energy efficient cluster based routing protocol for WSN using butterfly optimization algorithm and ant colony optimization," *Ad Hoc Netw.*, vol. 110, Art no. 102317,

- Jan. 2021, doi: 10.1016/j.adhoc.2020.102317.
- [24] S. M. M. H. Daneshvar, P. Alikhah Ahari Mohajer, and S. M. Mazinani, "Energy-efficient routing in WSN: A centralized cluster-based approach via grey wolf optimizer," *IEEE Access*, vol. 7, pp. 170019–170031, Nov. 2019, doi: 10.1109/ACCESS.2019.2955993.
- [25] Y. Li, B. Zhang, and S. Chai, "An energy balanced-virtual force algorithm for mobile-WSNs," in *IEEE International Conference on Mechatronics and Automation (ICMA)*, pp. 1779–1784, 2015. doi: 10.1109/ICMA.2015.7237755.
- [26] N. A. Ab. Aziz, A. W. Mohemmed, M. Y. Alias, K. Ab. Aziz, and S. Syahali, "Coverage maximization and energy conservation for mobile wireless sensor networks: A two phase particle swarm optimization algorithm," in *Sixth International Conference on Bio-Inspired Computing: Theories and Applications*, pp. 64–69, 2011. doi: 10.1109/BIC-TA.2011.6.
- [27] P. Cheng, C.-N. Chuah, and X. Liu, "Energy-aware node placement in wireless sensor networks," in *IEEE Global Telecommunications Conference*, vol. 5, pp. 3210–3214, 2004. doi: 10.1109/GLOCOM.2004.1378943.
- [28] A. Tripathi, H. P. Gupta, T. Dutta, R. Mishra, K. K. Shukla, and S. Jit, "Coverage and connectivity in WSNs: A survey, research issues and challenges," *IEEE Access*, vol. 6, pp. 26971–26992, 2018, doi: 10.1109/ACCESS.2018.2833632.
- [29] S. Das and M. K. Debbarma, "A survey on coverage problems in wireless sensor network based on monitored region," in *Advances in Data and Information Sciences*, pp. 349–359, 2019. doi: 10.1007/978-981-13-0277-0_29.
- [30] A. Boualem, M. Ayaida, and C. De Runz, "Semi-deterministic deployment based area coverage optimization in mobile WSN," in *IEEE Global Communications Conference (GLOBECOM)*, pp. 1–6, 2021. doi: 10.1109/GLOBECOM46510.2021.9685760.
- [31] A. Boualem, Y. Dahmani, A. Maatoug, and C. Derunz, "Area coverage optimization in wireless sensor network by semi-random deployment," in *Proceedings of the 7th International Conference on Sensor Networks*, pp. 85–90, 2018. doi: 10.5220/0006581900850090.
- [32] Z. Wang, H. Xie, Z. Hu, D. Li, J. Wang, and W. Liang, "Node coverage optimization algorithm for wireless sensor networks based on improved grey wolf optimizer," *Journal of Algorithms & Computational Technology*, vol. 13, pp. 1–15, Jan. 2019, doi: 10.1177/1748302619889498.
- [33] N.-T. Nguyen and B.-H. Liu, "The mobile sensor deployment problem and the target coverage problem in mobile wireless sensor networks are NP-hard," *IEEE Systems Journal*, vol. 13, no. 2, pp. 1312–1315, Jun. 2019, doi: 10.1109/JSYST.2018.2828879.
- [34] Y. Yoon and Y.-H. Kim, "An efficient genetic algorithm for maximum coverage deployment in wireless sensor networks," *IEEE Trans. Cybern.*, vol. 43, no. 5, pp. 1473–1483, Oct. 2013, doi: 10.1109/TCYB.2013.2250955.
- [35] S. K. Gupta, P. Kuila, and P. K. Jana, "Genetic algorithm approach for k-coverage and m-connected node placement in target based wireless sensor networks," *Comput. Electr. Eng.*, vol. 56, pp. 544–556, Nov. 2016, doi: 10.1016/j.compeleceng.2015.11.009.
- [36] Y. Yue, L. Cao, and Z. Luo, "Hybrid artificial bee colony algorithm for improving the coverage and connectivity of wireless sensor networks," *Wireless Pers. Commun.*, vol. 108, no. 3, pp. 1719–1732, Oct. 2019, doi: 10.1007/s11277-019-06492-x.
- [37] C.C. Yang and J.H. Wen, "A hybrid local virtual force algorithm for sensing deployment in wireless sensor network," in *Seventh International Conference on Innovative Mobile and Internet Services in Ubiquitous Computing*, pp. 617–621, 2013. doi: 10.1109/IMIS.2013.109.
- [38] Y. Zou and K. Chakrabarty, "Sensor deployment and target localization in distributed sensor networks," *ACM Trans. Embed. Comput. Syst.*, vol. 3, no. 1, pp. 61–91, Feb. 2004, doi: 10.1145/972627.972631.
- [39] A. Howard, M. J. Matarić, and G. S. Sukhatme, "Mobile sensor network deployment using potential fields: A distributed, scalable solution to the area coverage problem," in *Distributed Autonomous Robotic Systems 5*, pp. 299–308, 2002. doi: 10.1007/978-4-431-65941-9_30.
- [40] X. Wang, S. Wang, and D. Bi, "Virtual force-directed particle swarm optimization for dynamic deployment in wireless sensor networks," in *Advanced Intelligent Computing Theories and Applications with Aspects of Theoretical and Methodological Issues*, pp. 292–303, 2007. doi: 10.1007/978-3-540-74171-8_29.
- [41] M. Song, L. Yang, W. Li, and T. A. Gulliver, "Improving wireless sensor network coverage using the VF-BBO algorithm," in *IEEE Pacific Rim Conference on Communications, Computers and Signal Processing (PACRIM)*, pp. 318–321, 2013. doi: 10.1109/PACRIM.2013.6625496.
- [42] K. S. Umadevi, V. Shah, and U. Desai, "Node deployment using virtual force with particle swarm optimization in WSN," *Adv. Sci. Lett.*, vol. 24, no. 8, pp. 6017–6019, Aug. 2018, doi: 10.1166/asl.2018.12238.
- [43] X. Deng, Z. Yu, R. Tang, X. Qian, K. Yuan, and S. Liu, "An optimized node deployment solution based on a virtual spring force algorithm for wireless sensor network applications," *Sensors*, vol. 19, no. 8, Art. no. 1817, Jan. 2019, doi: 10.3390/s19081817.
- [44] J. Xie, D. Wei, S. Huang, and X. Bu, "A sensor deployment approach using improved virtual force algorithm based on area intensity for multisensor networks," *Math. Probl. Eng.*, vol. 2019, Art. no. e8015309, Feb. 2019, doi: 10.1155/2019/8015309.
- [45] S. Wang, X. Yang, X. Wang, and Z. Qian, "A virtual force algorithm-lévy-embedded grey wolf optimization algorithm for wireless sensor network coverage optimization," *Sensors*, vol. 19, no. 12, Art. no. 2735, Jan. 2019, doi: 10.3390/s19122735.
- [46] S. Liu, R. Zhang, and Y. Shi, "Design of coverage algorithm for mobile sensor networks based on virtual molecular force," *Comput. Commun.*, vol. 150, pp. 269–277, Jan. 2020, doi: 10.1016/j.comcom.2019.11.001.
- [47] X. Qi, Z. Li, C. Chen, and L. Liu, "A wireless sensor node deployment scheme based on embedded virtual force resampling particle swarm optimization algorithm," *Appl. Intell.*, vol. 52, pp. 7420–7441, Sep. 2021, doi: 10.1007/s10489-021-02745-0.
- [48] Y. Yao, Y. Li, D. Xie, S. Hu, C. Wang, and Y. Li, "Coverage enhancement strategy for WSNs based on virtual force-directed ant lion optimization algorithm," *IEEE Sens. J.*, vol. 21, no. 17, pp. 19611–19622, Sep. 2021, doi: 10.1109/JSEN.2021.3091619.
- [49] Q. Wen, X. Zhao, Y. Cui, Y. Zeng, H. Chang, and Y. Fu, "Coverage enhancement algorithm for WSNs based on vampire bat and improved virtual force," *IEEE Sens. J.*, vol. 22, no. 8, pp. 8245–8256, Mar. 2022, doi: 10.1109/JSEN.2022.3159649.
- [50] N. Bartolini, G. Bongiovanni, T. F. La Porta, and S. Silvestri, "On the vulnerabilities of the virtual force approach to mobile sensor deployment," *IEEE Trans. Mob. Comput.*, vol. 13, no. 11, pp. 2592–2605, Nov. 2014, doi: 10.1109/TMC.2014.2308209.

- [51] T. E. Kalayci and A. Uğur, "Genetic algorithm-based sensor deployment with area priority," *Cybern. Syst.*, vol. 42, no. 8, pp. 605–620, Nov. 2011, doi: 10.1080/01969722.2011.634676.
- [52] H. Mahboubi and A. G. Aghdam, "Distributed deployment algorithms for coverage improvement in a network of wireless mobile sensors: Relocation by virtual force," *IEEE Trans. Control. Netw. Syst.*, vol. 4, no. 4, pp. 736–748, Dec. 2017, doi: 10.1109/TCNS.2016.2547579.
- [53] M. Abo-Zahhad, S. M. Ahmed, N. Sabor, and S. Sasaki, "Utilisation of multi-objective immune deployment algorithm for coverage area maximisation with limit mobility in wireless sensors networks," *IET Wirel. Sens. Syst.*, vol. 5, no. 5, pp. 250–261, Oct. 2015, doi: 10.1049/iet-wss.2014.0085.
- [54] A. Osmani, M. Dehghan, H. Pourakbar, and P. Emdadi, "Fuzzy-based movement-assisted sensor deployment method in wireless sensor networks," in *First International Conference on Computational Intelligence, Communication Systems and Networks*, pp. 90–95, 2009. doi: 10.1109/CICSYN.2009.97.
- [55] F. Tossa, W. Abdou, E. C. Ezin, and P. Gouton, "Improving coverage area in sensor deployment using genetic algorithm," in *Computational Science – ICCS 2020*, pp. 398–408, 2020. doi: 10.1007/978-3-030-50426-7_30.



Vahid Kiani received his M.S. and Ph.D. degrees in Computer Engineering from Ferdowsi University of Mashhad (FUM), Mashhad, Iran, in 2011 and 2016, respectively. In 2017, he joined University of Bojnord as an Assistant Professor in the Department of Computer Engineering. His current research

interests include machine learning, data mining, digital image processing, and wireless sensor networks.



Azadeh Soltani received the B.S., M.S, and Ph.D. degrees in computer engineering from Ferdowsi University of Mashhad, Mashhad, Iran, in 2001, 2004, and 2014, respectively. She was a lecturer at Azad University of Bojnord from 2004 to 2006. She is currently an assistant professor in the Department of Computer Engineering at University of Bojnord, Bojnord, Iran. Her current

research interests include machine learning, data mining, and evolutionary algorithms.